Role of potential structure in the collisional excitation of metastable O(^1D) atoms

D. A. Padmavathi and Manoj K. Mishra
Department of Chemistry, Indian Institute of Technology, Powai, Bombay 400 076, India

Herschel Rabitz
Department of Chemistry, Princeton University, Princeton, New Jersey 08544

(Received 22 February 1993)

This paper considers the collisional excitation of O(^1D) modeled by the crossing of two valence $1\,^3\Pi_g$ curves dissociating to O(^3P)+O(^3P) [$V_{11}(R)$] and O(^3P)+O(^1D) [$V_{22}(R)$] which in turn are further crossed by the $C\,^3\Pi_g$ Rydberg curve dissociating to O(^3P)+O(^5S) [$V_{33}(R)$]. The role of structure in the potential curves and coupling matrix elements is quantitatively probed by the first-order functional-sensitivity densities $\delta \ln\sigma_{12}(E)/\delta \ln V_{ij}(R)$ of the excitation cross section $\sigma_{12}(E)$ obtained from close-coupling calculations. The results reveal that, in spite of the well-separated nature of the crossing between the two valence curves from their crossings with the Rydberg potential curve, the excitation cross section σ_{12} displays considerable sensitivity to the Rydberg curve $V_{33}(R)$ at all energies in the range 3.0–9.0 eV. For relative collisional energies corresponding to the higher closely spaced vibrational energy levels of the Rydberg state, the excitation cross section is found to be much more sensitive to the Rydberg state than to the two valence states themselves. At all energies, the sensitivity of the excitation cross section σ_{12} to the coupling $V_{12}(R)$ between the valence states is much larger than the sensitivity to the couplings $V_{13}(R)$ or $V_{23}(R)$ with the Rydberg state. At higher energies, the large increase in the sensitivity of the cross section to the Rydberg potential is mirrored by a similar increase in sensitivity to its coupling $V_{23}(R)$ with the upper valence state. Due to the weak coupling between the three curves, a qualitative similarity exists between the sensitivity profiles and those predicted by the Landau-Zener-Stueckelberg (LZS) theory. Quantitative departures witnessed in earlier work are, however, more pronounced for the multilevel curve crossings investigated here. Implications of the results for attempts to extend the LZS-type treatment to multilevel curve crossings and for functional-sensitivity-based algorithms for the inversion of cross-section data are discussed.

PACS number(s): 34.20.−b, 31.20.−d

I. INTRODUCTION

The interaction of the $C\,^3\Pi_g$ Rydberg state of O_2 with its two $1\,^3\Pi_g$ valence states dissociating to O(^3P)+O(^3P)[$V_{11}(R)$] and O(^3P)+O(^1D)[$V_{22}(R)$], respectively, has received extensive theoretical [1–3] and experimental [1–6] attention. The collisional excitation O(^3P)+O(^3P)→O(^3P)+O(^1D) is believed to be a significant source of red line emission in the outer atmosphere and has been modeled [1] by the crossing of the valence curves $V_{11}(R)$ and $V_{22}(R)$ with each other and the $C\,^3\Pi_g$ Rydberg curve $V_{33}(R)$. Even though the crossing between the valence curves $V_{11}(R)$ and $V_{22}(R)$ is well removed from their crossings with the Rydberg curve $V_{33}(R)$, the effect of the closed Rydberg channel on the excitation cross section $\sigma_{12}(E)$ is clearly seen [1] as resonances in the profile of the $|S^l_{12}|^2$ as a function of the nuclear angular momentum l. Since these resonances occur for small l values, the effect of the Rydberg curve on excitation cross sections has been taken to be insignificant [1].

While the qualitative reasoning employed above is plausible, the dynamical dependence of collision cross sections on the functional form of the underlying potential-energy curve(s) or surface(s) $V(R)$ may be examined through a first-order functional expansion of the collision cross section $\sigma([V])$,

$$\delta\sigma=\sigma([V+\delta V])-\sigma([V])\simeq\int dR\,\frac{\delta\sigma}{\delta V(R)}\delta V(R)\ , \qquad (1)$$

where R denotes generic coordinate space variables.

Those regions of R where $\delta\sigma/\delta V(R)$ is large (small) imply regions of importance (unimportance) for the cross section. Additionally, the sign dependence of the sensitivities tells the sense of how σ will respond to an increase or decrease in $V(R)$. While such an investigation may also be considered using the brute force method of varying $V(R)$ and repeating the calculations for the cross section many times, direct calculation of the functional sensitivities $\delta\sigma/\delta V(R)$ requires only a minor extension and expense beyond the cross-section calculation [10] alone. This approach has been applied to determine regions of potential curves critical to diverse dynamical processes [7–11].

In our earlier analyses using functional-sensitivity densities from close-coupling calculations [7,8] a qualitative similarity to the idealized $\delta(R-R^*)$-type behavior for $\delta\sigma_{12}(E)/\delta V_{12}(R)$ and the $\pm d\delta(R-R^*)/dR$-type behavior for $\delta\sigma_{12}(E)/\delta V_{11}(R)$ and $\delta\sigma_{12}(E)/\delta V_{22}(R)$ pointing to the critical importance of the curve crossing point (R^*) conformed to the predictions of the weak-coupling Landau-Zener-Stueckelberg (LZS) theory [12].

The area of importance of all the potential curves was, however, found to be much larger than the span of the loosely defined avoided crossing region or the transition width prescribed by the LZS theory [13] even for the weakly coupled systems. For systems with strong coupling [8,9] there was little resemblance between the sensitivity results and those predicted by the LZS theory. These analyses were, however, limited to systems modeled by the coupling of only two electronic levels. While the use of only two electronic states in the description of nonadiabatic transitions is generally reasonable [14,15], many collisions involve coupling of three or more electronic levels [1,15,16] and the attempts continue to extend the LZS-type description to such cases. These methods have, however, been applied only to model systems with constant couplings [15,16] and the tacit assumption of localized transition regions needs to be probed. Thus a functional-sensitivity analysis for a realistic three-state nonadiabatic system would be important to isolate the potential features controlling the dynamics. The use of functional-sensitivity densities as the kernel of an inversion algorithm is emerging as a powerful tool for the extraction of potentials and coupling matrix elements from spectroscopic and cross-section data [16]. An analysis of the functional-sensitivity profiles for three level systems should also be useful in the refinement of these inversion algorithms for extension into the multilevel nonadiabatic regime.

This paper analyzes the role of structure in potential-energy curves and the coupling matrix elements on the collisional excitation of $O(^1D)$ modeled by the three crossing curves [1]. The results are discussed in Sec. II and finally some concluding remarks are offered in Sec. III.

II. RESULTS AND DISCUSSION

The three potential curves used to model the collisional excitation $O(^3P)+O(^3P)\rightarrow O(^3P)+O(^1D)$ are displayed in Fig. 1. The potential curves and the coupling matrix elements are the same as those employed by Sun and Dalgarno [1].

The total inelastic cross section $\sigma_{12}(E)$ for the present case involving the collision of two identical Bosonic atoms is given by [1]

$$\sigma_{12}=\frac{2g_1\pi}{k_1^2}\sum_{l}^{\infty}(2l+1)|\mathbf{S}_{12}^{l}|^2 , \tag{2}$$

where g_1 is the probability that the atoms approach in channel 1 and the summation is limited to even values of l. The functional-sensitivity densities [8–11],

$$\frac{\delta\sigma_{12}(E)}{\delta V_{ij}(R)}=\frac{2g_1\pi}{k_1^2}\sum_{l}(2l+1)\mathrm{Re}\left[[\mathbf{S}_{12}^{l}(E)]^*\frac{\delta\mathbf{S}_{12}^{l}(E)}{\delta V_{ij}(R)}\right] , \tag{3}$$

at the nth point R_n on the solution grid are given by

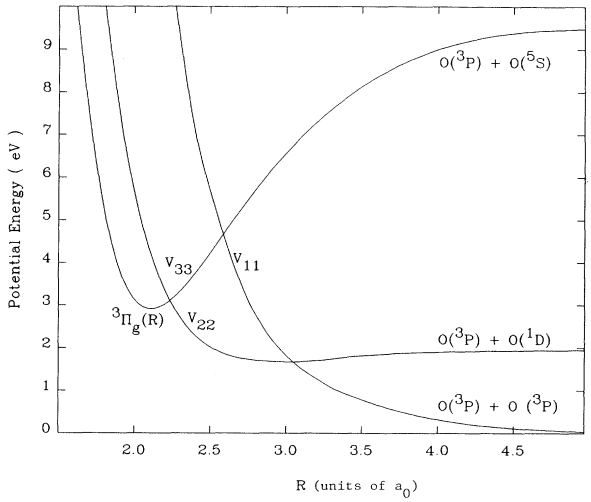

FIG. 1. The diabatic potentials $V_{11}(R)$, $V_{22}(R)$, and $V_{33}(R)$ for calculation of the total excitation cross section $\sigma_{12}(E)$ for the process $O(^3P)+O(^3P)\rightarrow O(^1D)+O(^3P)$. The lower valence potential curve $V_{11}(R)$ crosses the $^3\Pi_g$ Rydberg level $V_{33}(R)$ at $2.5885a_0$. The upper valence level $V_{22}(R)$ crosses the Rydberg level at $2.235a_0$. The two valence levels cross at $R^*=3.046a_0$. These curves are identical to those used to calculate $\sigma_{12}(E)$ in Ref. [1].

$$\frac{\delta\sigma_{12}(E)}{\delta V_{ij}(R_n)}=\frac{8g_1\pi^2}{k_1^2}\sum_{l}(2l+1)\times\mathrm{Im}[(\mathbf{S}_{12}^{l})^*\mathbf{U}_n^{l+}(i,2)\mathbf{U}_n^{l+}(j,1)] , \tag{4}$$

where U^{l+} is the outgoing wave function. Equation (4) serves as our working equation for the computation of sensitivities reported below.

The square of the scattering matrix element $|\mathbf{S}_{12}^{l}|^2$ as a function of the nuclear angular-momentum quantum number l at a relative energy of 4.16 eV has been plotted in Fig. 2. This figure is identical to a similar figure in Ref. [1] and the effect of the closed Rydberg channel as resonances in the $|\mathbf{S}_{12}^{l}|^2$ profile is clearly seen. The greatest contributions to the excitation cross section are from the l values in the vicinity of 150. The sharp resonant structures due to the closed Rydberg channel occur for small l values and therefore do not contribute significantly to the total excitation cross section [1]. The value of l^* associated with the maximum in the $|\mathbf{S}_{12}^{l}|^2$ profile corresponds to kR^*, where R^* is the internuclear distance at which the two valence levels $V_{11}(R)$ and $V_{22}(R)$ cross. The value of R corresponding to the resonant l values cannot be obtained from this kind of classical reasoning and indicates the quantum and nonlinear nature of the influence of the Rydberg level on the collisional outcome.

The total excitation cross section $\sigma_{12}(E)$ as a function of the relative collisional energy is plotted in Fig. 3. The oscillatory feature seen here is not well resolved in the

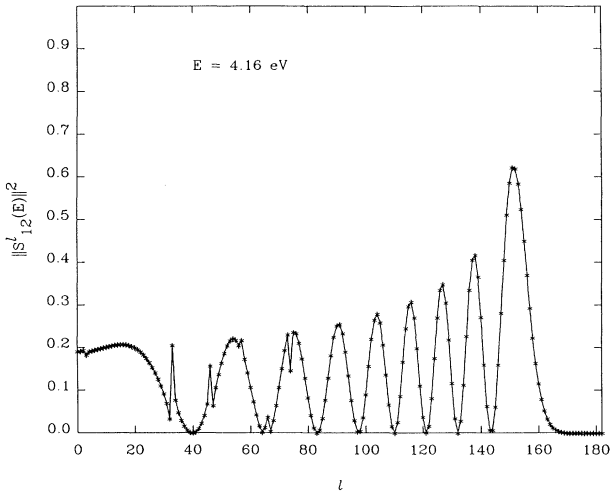

FIG. 2. The square of the scattering matrix element $|\mathbf{S}^l_{12}|^2$ as a function of the nuclear angular-momentum quantum number l at a relative energy of 4.16 eV. The effect of the closed Rydberg channel as resonances in the $|\mathbf{S}^l_{12}|^2$ profile is clearly seen. However, while the l^* clearly corresponds to kR^*, the value of R corresponding to the resonant l values cannot be obtained from this kind of linear classical reasoning.

equivalent plot of Ref. [1]. The oscillations begin at values of E lower than the Rydberg state minimum and have the same general energy dependence seen in the resonant scattering off shallow wells [18]. Such a well in $V_{22}(R)$ is indeed seen in Fig. 1. Thus, from this argument alone, the impact of the third Rydberg level at lower energies is expected to be small. The oscillatory structure is lost for energies higher than or approaching the value at the crossing between $V_{33}(R)$ and $V_{22}(R)$.

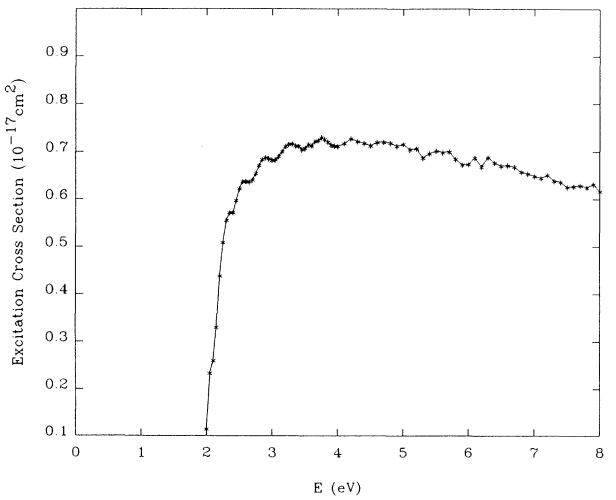

FIG. 3. The ^1D excitation cross-section profile $\sigma_{12}(E)$ as a function of the relative collisional energy. The oscillatory structure begins at E values much below the Rydberg minimum and corresponds to resonances in scattering off the shallow well in the upper valence curve $V_{22}(R)$. The resonant structure disappears at higher energies due to additional influence of the Rydberg level.

The log normalized functional-sensitivity derivatives $\delta \ln\sigma_{12}(E)/\delta \ln V_{ij}(R)$ can assess the *relative* importance of different potential curves as well as that of different regions in these curves to the collision cross section. Using long normalized functional-sensitivity densities, we can easily determine if the cross section is more sensitive to variations in a particular potential-energy curve or whether the coupling matrix element is the more important input. The functional-sensitivity densities $\delta \ln\sigma_{12}(E)/\delta \ln V_{ij}(R)$ for various values of the total collision energy are plotted in Fig. 4. At all energies the collision cross section $\sigma_{12}(E)$ is much more sensitive to the potentials than the coupling matrix elements and signifies a weakly coupled system [1–6,8]. At energies lower than that for the crossing between the lower valence curve $V_{11}(R)$ and $V_{33}(R)$ [e.g., for $E=3.30$ eV, the energy corresponding to the first excited vibrational level (see Table I) of the Rydberg curve], the excitation cross section is much less sensitive to the Rydberg curve as compared to the two valence curves, but is still more sensitive to the Rydberg curve than to the coupling between the two valence curves. The sensitivity of $\sigma_{12}(E)$ to the couplings $V_{13}(R)$ and $V_{23}(R)$ of the Rydberg curve with the two valence curves is almost negligible at all energies except at $E=6.1$ eV corresponding to a resonance spike in the total excitation cross section versus energy profile of Fig. 3. This resonance at 6.1 eV therefore must be attributed to the participation of the Rydberg level.

For total collision energy $E=3.30$ eV, clear qualitative similarity exists between the Gaussian-like profile for $\delta \ln\sigma_{12}(E)/\delta \ln V_{12}(R)$ centered at the crossing point $R^*(3.046a_0)$ and the idealized $\delta(R-R^*)$-type behavior prescribed by the LZS theory. Similarly, the $\pm d\delta(R-R^*)/dR$-type behavior with $\delta \ln\sigma_{12}(E)/\delta \ln V_{11}(R) \simeq -\delta \ln\sigma_{12}(E)/\delta \ln V_{22}(R)$ near $R \simeq R^*$ is in conformity with the prescription of the LZS theory found in the earlier analyses of weakly coupled systems [7,8]. This idealized behavior for $\delta \ln\sigma_{12}(E)/\delta \ln V_{11}(R)$ is lost at $E=6.1$ eV corresponding to a resonance spike in Fig. 3. The unusually large internuclear distance over which $\delta \ln\sigma_{12}(E)/\delta \ln V_{11}(R)$ is significant for this energy and the fact that this span is much larger than that for

TABLE I. Rydberg vibrational level energies in eV for $l=0$ with respect to $O(^3P)+O(^3P)$ level.

v	Theory Ref. [2]	Experiment Ref. [4]
0	3.037	3.038(10)
1	3.269	3.261(14)
2	3.498	3.488(12)
3	3.722	3.718(10)
4	3.942	3.933(15)
5	4.158	4.168(15)
6	4.370	4.388(15)
7	4.578	4.598(15)
8	4.781	4.800(20)
9	4.981	5.015(?)

$\delta \ln\sigma_{12}(E)/\delta \ln V_{22}(R)$ points to a strong role for the Rydberg level. This behavior clearly brings into question the notion of a uniform and localized transition region central to all generalized LZS-type treatments.

While the dominance of $\delta \ln\sigma_{12}(E)/\delta \ln V_{12}(R)$ over $\delta \ln\sigma_{12}(E)/\delta \ln V_{13}(R)$ and $\delta \ln\sigma_{12}(E)/\delta \ln V_{23}(R)$ persists at all energies, for $E=4.60$ eV [i.e., the energy of the seventh vibrational level in the Rydberg well and where $V_{11}(R)$ and $V_{33}(R)$ cross] and at other higher energies the excitation cross section is much more sensitive to the features in the Rydberg level $V_{33}(R)$ than to the valence levels $V_{11}(R)$ and $V_{22}(R)$ directly involved in the collisional excitation. At each energy, the radial span of the sensitivity profile $\delta \ln\sigma_{12}(E)/\delta \ln V_{33}(R)$ corresponds to the internuclear distance of the corresponding highest accessible vibrational level in $V_{33}(R)$. For $E=9.0$ eV, a peak also appears near the crossing point R^* between the two valence curves. The fact that the large sensitivity does not translate into a similar impact on the excitation cross section as noted during the discussion of Fig. 3 is made explicable by Fig. 5, where once again many resonance spikes are seen in the $|\mathbf{S}^l_{12}|^2$ profile but the total cross section is dominated by the critical cutoff at $l^* \simeq kR^*$. The resonance structures again occur for l values much smaller than the l^* corresponding to the maximum in the $|\mathbf{S}^l_{12}|^2$ profile. Also, while we have $l^* \simeq kR^*$, no such linear classical correlation exists for the $\delta \ln\sigma_{12}(E)/\delta \ln V_{33}(R)$, $\delta \ln\sigma_{12}(E)/\delta \ln V_{13}(R)$ or $\delta \ln\sigma_{12}(E)/\delta \ln V_{23}(R)$. The richness and magnitude of structure for higher E values points to a bottling up of

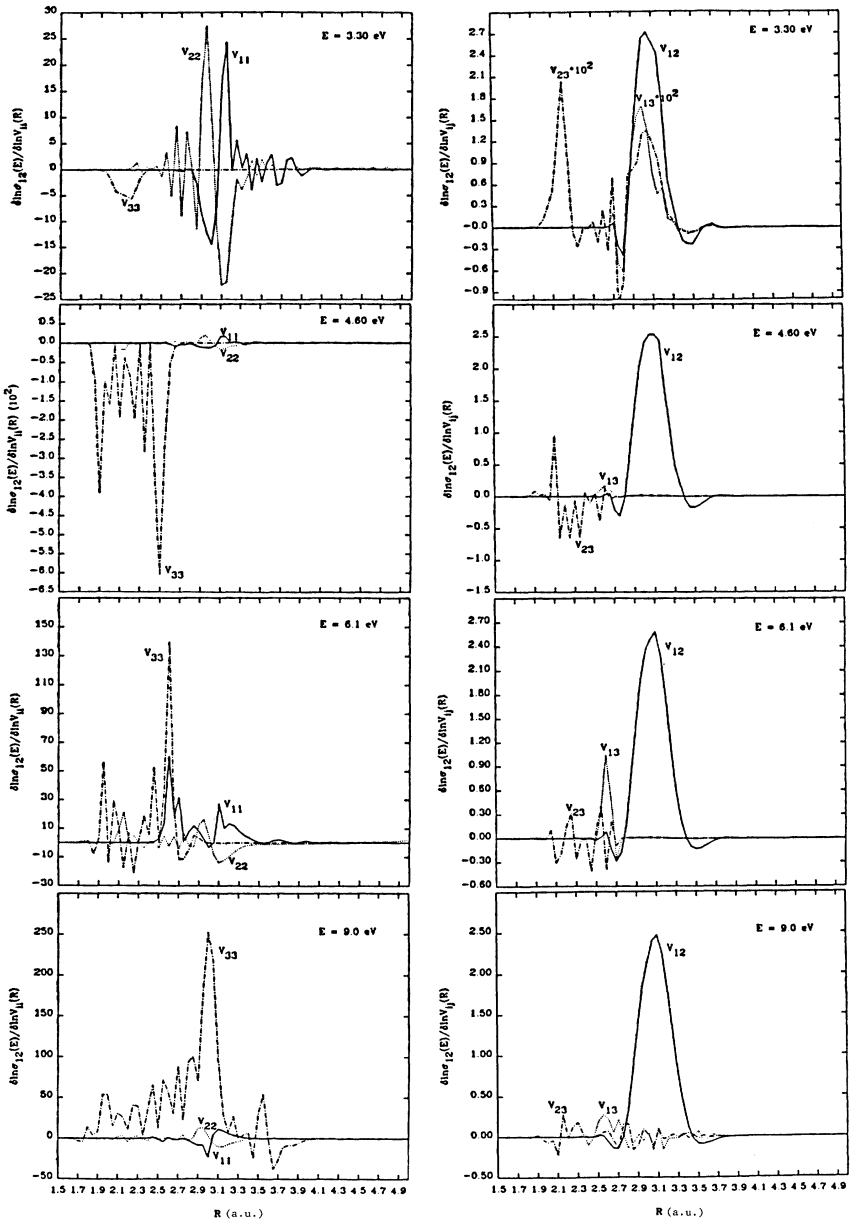

FIG. 4. Sensitivity profile $\delta \ln\sigma_{12}(E)/\delta \ln V_{ij}(R)$ for various values of the total relative collisional energy E. Highly nonlinear and nonclassical footprints of the closed Rydberg channel are clearly seen for higher energies. The correlated $\pm d\delta(R-R^*)/dR$-type behavior for the sensitivity profiles $\delta \ln\sigma_{12}(E)/\delta \ln V_{11}(R)$ and $\delta \ln\sigma_{12}(E)/\delta \ln V_{22}(R)$ in the vicinity of R^* and the Gaussian-type feature for $\delta \ln\sigma_{12}(E)/\delta \ln V_{12}(R)$ centered at R^* mimic the idealized $\delta(R-R^*)$ behavior predicted by the LZS theory at most energies. The domain of sensitivity, however, extends beyond the crossing region and has a strong dynamic dependence with different transition widths for $V_{11}(R)$ and $V_{22}(R)$ at $E=6.1$ eV and underscores the need to augment intuitive pictures rooted in the LZS theory.

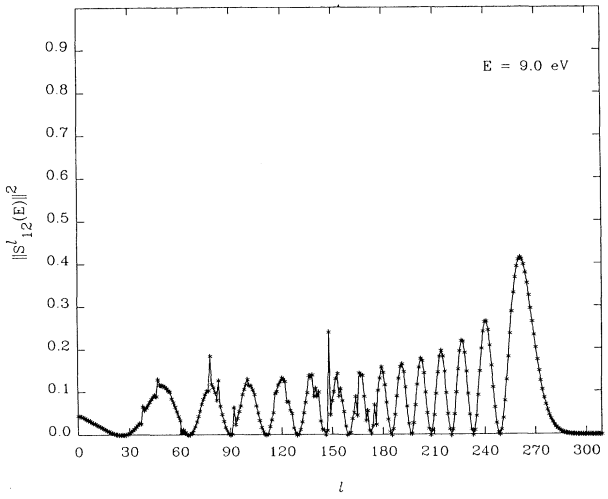

FIG. 5. Same as Fig. 2 but for $E=9.0$ eV.

the wave function between many turning points in the Rydberg well for these energies. From Fig. 1 we can see that these energies correspond to the further crossing of the Rydberg level by the lower valence level $V_{11}(R)$ ($E=4.6$ eV), resonance in the total excitation cross-section profile ($E=6.1$ eV), or availability of closely spaced, nearly degenerate vibrational levels in the Rydberg curve ($E=9.0$ eV). We believe this bottling up of the wave function in the Rydberg well at higher energies is responsible for the large magnitude of $\delta \ln\sigma_{12}(E)/\delta \ln V_{33}(R)$ at these energies. This would be in accord with our earlier finding that the sensitivities for the two-level case increases with a decrease in energy [7,8] (i.e, there is more "time" to sample the features of the potential curves). In any case, there is a very strong dynamical dependence in the role of potential structure, and the notion of transition width prescribed by LZS theory [13] has little relevance in this context where widely different domains of sensitivities are seen for different potential curves.

III. CONCLUDING REMARKS

In this paper first-order functional-sensitivity derivatives were employed to gain insights into the comparative importance of various potential-energy curves and coupling matrix elements mediating a nonadiabatic collision involving multilevel curve crossings. The calculation of nonadiabatic collision cross sections using the generalized LZS-type extensions for systems with multi-level-curve crossings has so far been limited to those with constant coupling matrix elements and/or simple repulsive potential curves [15,16]. While the generalized LZS-type extensions have offered excellent agreement for many model systems, our results indicate that application of these methods to more realistic systems like the one treated here should offer interesting new insights in establishing them as general tools. The strong energy-dependent quantum interference behavior reflected in all the sensitivity profiles underscores the need to augment intuitive pictures rooted in LZS theory.

The use of sensitivity coefficients $\delta \ln\sigma_{12}(E)/\delta \ln V_{33}(R)$ in Eq. (1) points to an inherent nonlinearity in the influence of the Rydberg level on the collisional outcome. This implies that the domain of linearity in the present system is small and that an inversion algorithm based on first-order sensitivity densities [17] will need to utilize a large number of small step sizes in moving through the function space to extract $V_{33}(R)$ from cross-section data for this system.

ACKNOWLEDGMENTS

We are grateful to Professor A. Dalgarno for making available the diabatic potentials used in this work. M.K.M. is pleased to acknowledge many helpful discussions with Dr. Peter Gross. This investigation has been sponsored by the Board of Research in Nuclear Sciences of the Department of Atomic Energy, India, through their Grant No. 37/16/89-G to M.K.M. Their support is gratefully acknowledged. H.R. acknowledges support from the U.S. Department of Energy.

[1] Y. Sun and A. Dalgarno, J. Chem. Phys. **96**, 5017 (1992).
[2] R. S. Friedman, M. L. Du, and A. Dalgarno, J. Chem. Phys. **93**, 2375 (1990).
[3] R. S. Friedman and A. Dalgarno, J. Chem. Phys. **93**, 2370 (1990).
[4] W. J. van der Zande, W. Koot, and J. Los, J. Chem. Phys. **91**, 4597 (1989).
[5] W. J. van der Zande, W. Koot, J. R. Preston, and J. Los, Chem. Phys. **126**, 169 (1988).
[6] W. J. van der Zande, W. Koot, J. R. Preston, and J. Los, Chem. Phys. Lett. **140**, 175 (1987).
[7] M. Mishra, R. Guzman, and H. Rabitz, Phys. Rev. A **36**, 1124 (1987).
[8] D. A. Padmavathi, M. K. Mishra, and H. Rabitz, Phys. Rev. A **48**, 279 (1993).
[9] D. A. Padmavathi, M. K. Mishra, and H. Rabitz, J. Chem. Phys. (to be published).
[10] S. Shi and H. Rabitz, Comput. Phys. Rep. **10**, 1 (1989).
[11] M. J. Smith, S. Shi, and H. Rabitz, J. Chem. Phys. **91**, 1051 (1989).
[12] L. Landau, Sov. Phys. **2**, 46 (1932); C. Zener, Proc. R. Soc. London, Ser. A **137**, 696 (1933); E. C. G. Stueckelberg, Helv. Phys. Acta **5**, 369 (1932).
[13] M. S. Child, *Molecular Collision Theory* (Academic, London, 1974).
[14] R. D. Levine and R. B. Bernstein, *Molecular Reaction Dynamics and Chemical Reactivity* (Oxford University Press, New York, 1987).
[15] H. Nakamura, Int. Rev. Phys. Chem. **10**, 123 (1991) and references therein; H. Nakamura, J. Chem. Phys. **87**, 4031 (1987); H. Nakamura, J. Phys. Chem. **88**, 4812 (1984).
[16] For example, A. M. Wooley, Mol. Phys. **22**, 207 (1971); F.

J. McLafferty and T. F. George, J. Chem. Phys. **63**, 2609 (1975) and references therein; J. R. Laing and T. F. George, Phys. Rev. A **16**, 1082 (1977); U-I. Cho and B. C. Eu, Mol. Phys. **32**, 1 (1976); **32**, 19 (1976); B. C. Eu and N. Zaritsky, J. Chem. Phys. **70**, 4986 (1979); M. L. Sink and D. Bandrauk, *ibid.* **66**, 5313 (1976); H. J. Korsch, Mol. Phys. **49**, 325 (1983).

[17] T. S. Ho and H. Rabitz, J. Chem. Phys. **89**, 5614 (1988); **91**, 7590 (1989); **94**, 2305 (1991); **96**, 7092 (1992); H. Heo, T. S. Ho, K. Lehmann, and H. Rabitz, *ibid.* **97**, 852 (1992); R. Boyd, T. S. Ho, H. Rabitz, D. A. Padmavathi, and M. K. Mishra (unpublished).

[18] E. Merzbacher, *Quantum Mechanics* (Wiley, New York, 1970), p. 109.